

AD

AD-E402 725

Contractor Report ARPBM-CR-95001

**DEGREE OF MIXING ANALYSIS IN LOVA PROPELLANTS
BY WIDE-ANGLE X-RAY DIFFRACTION**

Dr. Rahmi Yazici
Dr. Dilhan M. Kalyon
Highly Filled Materials Institute
Stevens Institute of Technology
Castle Point on Hudson
Hoboken, New Jersey 07030

David Fair
Project Engineer
ARDEC

April 1996



US ARMY
TANK AUTOMOTIVE AND
ARMAMENTS COMMAND
ARMAMENT RDE CENTER

**U.S. ARMY ARMAMENT RESEARCH, DEVELOPMENT AND
ENGINEERING CENTER**

Production Base Modernization Activity

Picatinny Arsenal, New Jersey

Approved for public release; distribution is unlimited.

19960523 007

ORIG QUALITY INSURED

The views, opinions, and/or findings contained in this report are those of the authors(s) and should not be construed as an official Department of the Army position, policy, or decision, unless so designated by other documentation.

The citation in this report of the names of commercial firms or commercially available products or services does not constitute official endorsement by or approval of the U.S. Government.

Destroy this report when no longer needed by any method that will prevent disclosure of its contents or reconstruction of the document. Do not return to the originator.

| REPORT DOCUMENTATION PAGE | | | Form Approved OMB No. 0704-0188 | |
|--|--|--|---|-----------------------------------|
| Public reporting burden for this collection of information is estimated to average 1 hour per response, including the time for reviewing instructions, searching existing data sources, gathering and maintaining the data needed, and completing and reviewing the collection of information. Send comments regarding this burden estimate or any other aspect of this collection of information, including suggestions for reducing this burden, to Washington Headquarters Services, Directorate for Information Operation and reports, 1215 Jefferson Davis Highway, Suite 1204, Arlington, VA 22202-4302, and to the Office of Management and Budget, Paperwork Reduction Project (0704-0188), Washington, DC 20503. | | | | |
| 1. AGENCY USE ONLY (Leave blank) | | 2. REPORT DATE April 1996 | | 3. REPORT TYPE AND DATES COVERED |
| 4. TITLE AND SUBTITLE DEGREE OF MIXING ANALYSIS IN LOVA PROPELLANTS BY WIDE-ANGLE X-RAY DIFFRACTION | | | 5. FUNDING NUMBERS | |
| 6. AUTHOR(S) Dr. Rahmi Yazici and Dr. Dilhan M. Kalyon, Highly Filled Materials Institute David Fair, Project Engineer, ARDEC | | | | |
| 7. PERFORMING ORGANIZATION NAME(S) AND ADDRESSES(S) ARDEC, PBM Production Base Modernization Activity (AMSTIO-IRA-W) Picatinny Arsenal, NJ 21005-5001 | | | 8. PERFORMING ORGANIZATION REPORT NUMBER Highly Filled Materials Institute Stevens Institute of Technology Castle Point on Hudson Hoboken, New Jersey 07030 | |
| 9. SPONSORING/MONITORING AGENCY NAME(S) AND ADDRESS(S) ARDEC, DOIM Information Research Center (AMSTA-AR-IMC) Picatinny Arsenal, NJ 07806-5000 | | | 10. SPONSORING/MONITORING AGENCY REPORT NUMBER Contractor Report ARPBM-CR-95001 | |
| 11. SUPPLEMENTARY NOTES This project was accomplished as part of the U.S. Army's Production Base Modernization Activity. The primary objective of this program is to develop, on a timely basis, manufacturing processes, techniques, and equipment for use in production of Army material. To be published in part in Journal of Energetic Materials (accepted for publication in April 1995). | | | | |
| 12a. DISTRIBUTION/AVAILABILITY STATEMENT Approved for public release; distribution is unlimited. | | | 12b. DISTRIBUTION CODE | |
| 13. ABSTRACT (Maximum 200 words) Four different lots of LOVA propellants were analyzed to determine quantitatively the distributive mixing achieved by two continuous and two batch mixing processes. The degree of mixing distribution technique based on wide-angle x-ray diffractometry, which was developed with earlier funding of U.S. Army Production Base Modernization Activity, was successfully applied to assess and compare the four LOVA lots and the four processing methodologies applied. The quantitative degree-of-mixing parameters obtained through this work were also found to be amenable for prediction the propellant performance, i.e., the LOVA lot that failed the burn test in the field exhibited the lowest degree of mixing, whereas the LOVA lot that passed the burn test exhibited one of the highest degree of mixing in this investigation. The new technique has also been applied successfully in evaluation of other multi-component energetics and its potential for applicability as an on-line and on-site technique is suggested. | | | | |
| 14. SUBJECT TERMS Evaluation of propellants X-ray diffraction | | | 15. NUMBER OF PAGES 42 | |
| Degree-of-mixing RDX | | | 16. PRICE CODE | |
| Mixing distribution HMX | | | LOVA | |
| 17. SECURITY CLASSIFICATION OF REPORT UNCLASSIFIED | | 18. SECURITY CLASSIFICATION OF THIS PAGE UNCLASSIFIED | 19. SECURITY CLASSIFICATION OF ABSTRACT UNCLASSIFIED | 20. LIMITATION OF ABSTRACT SAR |

SUMMARY

Four different lots of LOVA propellants were analyzed to determine quantitatively the distributive mixing achieved by two continuous and two batch mixing processes. The degree of mixing distribution technique based on wide-angle x-ray diffractometry which was developed with earlier funding of US Army Production Base Modernization Activity was successfully applied to assess and compare the four LOVA lots and the four processing methodologies applied. The four LOVA lots that were analyzed were:

- 1) batch-mixed and ram extruded Batch-54 of Indian Head,
- 2) batch-mixed and ram extruded Batch-45 of Indian Head,
- 3) twin-screw pre-blended and twin-screw extruded TSE-TH1 of Longhorn (Thiokol),
- 4) batch pre-blended and twin-screw extruded TSE-IH1 of Indian Head.

Overall, the degree of mixing was highest in TSE-TH1 and Batch-54, and lowest in Batch-45, and TSE-IH1 lot falls in between. The distribution of plasticized CAB binder variation was closest to a symmetric and unimodal distribution in the TSE-TH1 lot. The plasticized CAB binder content was close to the target value in the Batch-54, Batch-45 and TSE-TH1 lots, but was 2% by volume higher in TSE-IH1 lot. The RDX content was 1% to 2% lower in TSE-TH1 and TSE-IH1 lots when compared to the Batch-54 and Batch-45 lots.

The quantitative degree-of-mixing parameters obtained through this work were also found to be amenable for predicting the propellant performance, i.e., the LOVA lot Batch-45 that failed the burn test in the field exhibited the lowest degree of mixing, whereas the LOVA lot Batch-54 that passed the burn test exhibited one of the highest degree of mixing in this investigation.

Although the scope of this report is focused on the statistical distribution of the mixing of the ingredients in a given LOVA lot, location-specific measurements on LOVA strands are also being carried out. The radial diffusion of the liquid ingredients in the propellant grains and free surfaces is currently being analyzed by microdiffraction methods.

The new technique has also been applied successfully in evaluation of other multi-component energetics; and its potential for applicability as an on-line and on-site technique is suggested.

CONTENTS

| | Page |
|---|------|
| Introduction | 1 |
| Program Goals | 2 |
| Experimental Procedures | 3 |
| Materials Processing and Sample Preparations | 3 |
| Characterization of the Mixing Indices | 4 |
| Background on the Analytical Technique: Wide-Angle X-Ray Diffractometry | 7 |
| Results and Discussions | 9 |
| Conclusions | 12 |
| Future Work | 14 |
| References | |
| Distribution List | |

TABLES

| | | |
|----|---|----|
| 1 | LOVA formulation | 15 |
| 2 | Mixing indices | 15 |
| 3a | LOVA ingredients | 16 |
| 3b | Crystal structure of LOVA ingredients | 16 |
| 4 | X-ray diffraction experimental parameters | 17 |
| 5 | Plasticized CAB statistical parameters at 10 sq. mm scale | 17 |
| 6 | RDX + HMX statistical parameters at 10 sq. mm scale | 17 |
| 7 | Plasticized CAB statistical parameters at 1 sq. mm scale | 18 |
| 8 | RDX + HMX statistical parameters at 1 sq. mm scale | 18 |

FIGURES

| | Page |
|---|------|
| 1 0.3" diameter LOVA grain (a), transverse section (b) | 19 |
| 2 Extruded LOVA propellant: sampling and x-ray probe size | 20 |
| 3 (a) Typical x-ray diffraction pattern of LOVA propellants | 21 |
| (b) Simulated bar pattern of crystalline RDX | 22 |
| (c) Simulated bar pattern of crystalline HMX | 22 |
| (d) Amorphous peak of plasticized CAB | 22 |
| 4 Deconvolution of a typical x-ray diffraction pattern of LOVA propellant where integrated areas of the peaks from different ingredients are marked | 23 |
| 5 Plasticized CAB variations in LOVA propellants at 10 sq. mm scale | 24 |
| 6 RDX + HMX variation in LOVA propellants at 10 sq. mm scale | 25 |
| 7a Plasticized CAB variation in LOVA propellants at 1 sq. mm scale | 26 |
| 7b Plasticized CAB variation distribution in LOVA propellants at 1 sq. mm scale | 27 |
| 8 RDX + HMX variation in LOVA propellants at 1 sq. mm scale | 28 |
| 9 Typical microstructures of (a) batch 54, (b) batch 45, (c) TSE-TH1, (d) TSE-IH1, and (e) binder deprived RDX-rich region of batch 45 | 29 |
| 10 Microvoid defect formation in LOVA lots TSE-TH1 (a and b) and batch 54 (c) | 30 |

INTRODUCTION

Solid propellant materials are used in critical applications which demand the delivery of controlled and sustainable thermo-chemical reactions for accurate propulsion. The energetic ingredients that go into solid propellants, such as the solid-phase fuel/oxidizers, polymeric fuel/binders and plasticizers; and others such as the catalyzers and wetting agents have to be metered accurately and mixed rigorously in order to secure a uniform microstructure and, thus, a uniform energetic behavior throughout the solid propellant. Inadequate mixing of the ingredients and formation of defects lead to production of inhomogeneous propellants with localized "sensitive" regions that seriously undermine the accuracy of the energetic performance.

Currently, "burn" tests are applied to assess the adequacy of a given propellant lot produced by a certain processing operation. A whole production lot could be discarded if found inadequate because of the stringent requirements. Since these tests are carried-out on final products, the material and monetary losses could be significant.

In order to reduce waste and to improve product quality and production safety, reliable analytical techniques need to be developed and employed for "degree of mixing" and defect distribution analysis in propellants that can be applied in processing environments and be amenable to on-line utilization.

The techniques applied to characterize the degree of the mixedness of a composite such as a propellant would involve either direct or indirect methods. Indirect methods include the determination of some representative property including transmissive, reflective, resistivity, ultrasound and rheological properties. Such techniques are suitable for product quality control, where the relationship between the measured property and the ultimate property of interest is a priori known. However, although such techniques are useful, they are post-mortem and provide no direct quantitative data on how well the ingredients are interspersed in each other.

Some techniques involving incorporation of color tracers are also available for study of degree of mixedness.¹⁻⁶ For example, Kalyon and co-workers^{7,8} have employed color incorporated thermoplastic elastomers, followed by computerized image analysis, to investigate the distributive mixing of thermoplastic elastomers in the regular flighted and kneading disc elements of twin-screw extruders. Although all these techniques are useful for understanding and modeling of the mixing process under different processing modes, their applicability in the production environment of propellants is highly limited.

On the other hand, the rapid advent of imaging and sensing technology has facilitated the introduction of various powerful techniques, including the nuclear magnetic resonance (NMR) imaging and x-ray based techniques, to the analyses of opaque mixtures. Sinton and Yazici et al.⁹ have employed magnetic resonance imaging, wide-angle x-ray diffraction and x-ray radiography to characterize the amount of air entrained into composite suspensions with elastomeric binders during extrusion processing, which is related principally to the degree of fill profile in the extruder. Yazici and Kalyon¹⁰ have developed and applied electron probe

and x-ray diffraction techniques to the analysis of degree of mixing in concentrated suspensions that were solid-propellant simulants continuously processed with a commercial twin-screw extruder.

In this study, the analytical technique based on wide-angle x-ray diffraction and developed by the authors to assess the degree of mixing in concentrated suspensions is applied to evaluate live propellants. The applicability of this technique to the quantitative characterization of the distributive mixing achieved in four LOVA propellant lots processed by continuous and batch mixing operations was demonstrated, comparatively. The investigation was carried out as an integral part of the processing design task of the Longhorn LOVA development program of the U.S. Army PBMA where various batch and continuous processing methods are being evaluated.

PROGRAM GOALS

Apply analytical methods based on wide-angle X-ray diffractometry to:

- identify various components in energetic LOVA formulations
- quantitatively determine the volume fraction of each component at various locations in energetic LOVA grains.
- quantitatively characterize the degree of mixing of each component in the grain at desired scales of examination
- develop a data base to assess the comparative state of mixedness of energetic LOVA samples prepared by different mixing and processing modes
- correlate processing/microstructure/performance relationships of energetic materials

EXPERIMENTAL PROCEDURES

Materials Processing and Sample Preparation

This investigation focused on a live LOVA formulation which consisted of approximately 30% by volume polymeric matrix and 70% by volume solids. Same formulation was used in all four continuous and batch mixing processes. The matrix of the low vulnerability formulation constituted cellulose acetate butyrate (CAB), an organic plasticizer, energetic ingredients and wetting agents. The solid content was primarily 2,4,6-cyclotrimethylene-trinitamine, or hexogen (RDX) for short, that contained few volume percent octahydro-1,3,5,7-tetranitro-1,3,5,7 tetrazocine, or octagon (HMX) for short, as a by-product of RDX synthesis. The average particle size of the RDX was 4 microns. There were other ingredients that will not be disclosed in this publication. The formulation of these LOVA propellants as permitted for this publication is summarized in Table 1, where the nominal volume fractions of the ingredients are listed.

Samples of the extruded propellant grains (see Figure 1) were acquired through U.S. Army Production Base Modernization Activity at Picatinny Arsenal. Both the continuous processed, i.e., twin-screw mixed and extruded, and the batch processed, i.e., batch mixed and ram extruded grains were 0.3" in diameter and contained internal perforations as seen in Figure 1. Four (4) different lots of LOVA propellants were analyzed to evaluate their degree of mixing distributions and microstructural integrity, comparatively. These lots were:

1) BATCH-54

Processed at: Indian Head by NSWC/IHDIV

Procedure: i) batch mixed
ii) ram extruded into propellant grains

Sample quantity: 3 grains

2) BATCH-45

Processed at: Indian Head by NSWC/IHDIV

Procedure: i) batch mixed
ii) ram extruded into propellant grains

Sample quantity: 3 grains

3) TSE-TH1

Processed at: Longhorn AAP by Thiokol

Procedure: i) preblend/premixed by twin screw extrusion
ii) granulated and remixed by twin screw extrusion, and

iii) twin-screw extruded into propellant grains

Sample quantity: 3 grains

4) TSE-IH1

Processed at: Indian Head by NSWG/IHDIV

Procedure: i) preblend by a batch process
ii) granulated and mixed by twin screw extrusion, and
iii) twin screw extruded into propellant grains

Sample quantity: 3 grains

There are distinct differences between batch mixing and continuous mixing processes. In batch mixing the total amount of each ingredient that goes into a lot according to the given formulation is pre-measured and added into the mixer in a given order. Once all the ingredients are added, the formulation is mixed for a certain amount of time using high-shear-rate-type mixing elements. In continuous mixing, however, the ingredients are added continuously in small but controlled feeding rates at various locations on the twin-screw extruder. The feeding rates of the ingredients are metered to have correct compositional fraction for each ingredient at any given time, and as prescribed by the formulation. In continuous mixing only a small volume of formulation is mixed at any given time in the mixing volume of the twin-screw extruder. The mixing in continuous processing is expected to be more uniform than batch mixing, because of the higher surface-to-volume ratios available and the ability to pass the materials repeatedly through small gaps exposing them to high shear stress values.

Individual strands or grains of the extruded propellants, each measured 0.3" in diameter and 1" long, were randomly chosen from the continuous processed TSE-TH1 and TSE-IH1, and batch processed Batch-45 and Batch-54 lots. Each grain was sectioned as shown in Figure 2, prior to characterization with x-ray diffraction. Sectioning was carried-out with a guillotine and a jeweler's saw followed by fine polishing with 600 grid wet emery paper. Some of the cross-sectional specimens for electron microscopy were prepared by fracturing of the extrudate grains. All the samples, the tools and the metal bench-top were electrically grounded in order to eliminate electrostatic build-up during sample preparation following the safety suggestions made by ONR's safety officer, Mr. Robert Zaleski, who inspected our facilities in May 9, 1994.

In addition to the processed propellant grains, samples of the raw ingredients that were used in the processing, i.e., CAB, plasticizer and RDX + HMX powder were also analyzed as reference materials.

Characterization of the Mixing Indices

Various mixing indices were derived from the statistical parameters of the experimental measurements and used to quantitatively characterize the degree of mixing of the four LOVA propellant lots. Wide-angle x-ray diffractometry (XRD) was used as the principal analytical

method.

The mixing indices were calculated at different scales of examination by varying the sampling area through alterations of the size of the x-ray probe by several orders of magnitude as shown in Figure 2. The relative volume-fractions of the solid ingredients and the binder was utilized as a measure of the degree of mixing of the samples, i.e., for binder volume fraction: plasticized CAB binder over CAB plus the other ingredients (RDX, HMX and "Others")

$$\frac{\phi_{\text{CAB}}}{\phi_{\text{CAB}} + \phi_{\text{RDX}} + \phi_{\text{HMX}} + \phi_{\text{others}}} \quad (1)$$

In general, the quantitative description of the mixing quality or goodness of mixing of a given mixture can be developed by comparison of the state of the mixture to the most complete mixing state attainable.¹¹ This complete mixing corresponds to statistical randomness of the ultimate properties of the ingredients being mixed which would follow the Binomial distribution.¹²

If one makes N measurements of concentration, c_i of one of the components, then the mean concentration may be calculated according to

$$\bar{c} = \frac{1}{N} \sum_{i=1}^N c_i, \quad (2)$$

where \bar{c} should not differ significantly from the overall concentration of the component, ϕ , unless a faulty sampling technique is used. The difference between \bar{c} and ϕ decreases as the number of the characterized samples N, is increased. The measured concentration values of the minor component also depend on the sample size. These values approach the overall concentration of the minor component ϕ as the sample size is increased.

A basic measure of the homogeneity of a mixture is the extent to which the concentration values at various regions of the volume of the mixture differ from the mean concentration. The variance s^2 , arising from the individual concentration c_i measurements, provides such an index to quantitatively assess the degree of mixedness. The variance is given by

$$s^2 = \frac{1}{(N-1)} \sum_{i=1}^N (c_i - \bar{c})^2. \quad (3)$$

A small variance implies that most of the samples yield concentration c_i values which are close to the mean \bar{c} of all samples, thus suggesting a homogeneous system. The

deviation of the sample measurements from the mean \bar{c} is given by standard deviation

$$s = \sqrt{s^2} \quad (4)$$

which is defined as the square root of the variance, and is in the same units as the concentration data. When the means of two concentration data sets differ greatly, a measure of relative variability is defined with coefficient of variation, v , which is the ratio of standard deviation to mean¹³

$$v = \frac{s}{\bar{c}} \quad (5)$$

The maximum variance occurs if the components are completely segregated. Maximum variance is given by

$$s_0^2 = \bar{c}(1-\bar{c}). \quad (6)$$

If the variance is normalized to its maximum value, the resulting parameter is called the intensity of segregation, I_{seg} .^{11,12} This is given by

$$I_{\text{seg}} = \frac{s^2}{s_0^2} = \frac{s^2}{\bar{c}(1-\bar{c})}. \quad (7)$$

One can define the intensity of mixing as:

$$I_{\text{mix}} = 1 - \frac{s^2}{s_0^2} \quad (8)$$

A distributive mixing index, MI, can be defined as:

$$MI = 1 - \frac{s}{s_0} \quad (9)$$

Both the intensity of mixing and the mixing index values range from zero, for completely segregated system, to one, for ideally homogeneous system.

In this study, it was found that coefficient of variation (v), intensity of mixing (I_{mix}) and mixing index (MI) are all additional important indices in evaluating goodness or distribution of mixing. The mixing indices and the statistical parameters used in this work are summarized in Table 2.

Background on the Analytical Technique: Wide-Angle X-Ray Diffractometry

X-ray diffractometry has been successfully applied for both qualitative and quantitative phase analysis in multi-phase materials.^{14,15} Upon irradiation with x-rays, a given substance produces a characteristic diffraction pattern. Diffraction is essentially a scattering phenomenon in which a large number of atoms (or molecules) in the crystalline material, arranged periodically on a lattice, scatter the x-rays in phase. These phase relations are such that destructive interference occurs in most directions of scattering; but in a few directions constructive interference takes place and diffracted beams are formed. According to Bragg Law, the diffracted beams make a 2θ angle with respect to the incident beam, i.e.

$$\lambda = 2d \sin \theta, \quad (11)$$

where λ is the wavelength of the x-rays of the incident beam and d is the spacing between the atomic (lattice) planes of the crystalline material which make a θ angle with respect to the incident beam. Since the d -spacings between atomic planes and their distribution in space (the crystal structure) is unique for each material, the angular distribution of the diffraction peaks and their intensities (the diffraction pattern) is also unique for a particular material. Qualitative analysis by x-ray diffraction is accomplished by identification of the particular diffraction pattern of a substance from the standard diffraction tables.¹⁶

The particular advantage of x-ray diffraction analysis is that it discloses the presence of a substance, as that substance actually exists in the sample, and not in terms of its constituent chemical elements. If the sample contains more than one compound or phase that constitute the same chemical elements, all these compounds are disclosed by diffraction analysis. Quantitative analysis is also possible, because the intensity of the diffraction pattern of a particular phase - in a mixture of phases - depends on the concentration of that phase in the mixture. The relation between the integrated intensity I_x and the volume fraction ϕ_x of a phase is generally nonlinear since diffracted intensity depends strongly on the absorption coefficient of the mixture, μ_m , which itself depends on the concentration. For a two-phase material, (with absorption coefficients μ_1 and μ_2 for the individual phases) the absorption coefficient for the mixture becomes:

$$\mu_m = \phi_1 \mu_1 + \phi_2 \mu_2. \quad (12)$$

The integrated intensity from phase 1 is then given by:¹⁵

$$I_1 = K_1 \phi_1 / \mu_m, \quad (13)$$

where K_1 is a constant that depends on the material and the incident beam used but not on the concentration. The relative ratio of intensities from phases 1 and 2, however, is independent of μ_m and varies with concentration

$$\frac{I}{I_1 + I_2} = \frac{K_1 \phi_1}{K_1 \phi_1 + K_2 \phi_2} \quad (14)$$

Where the K values can be determined either from the I_x/I_{corundum} values listed by JCPDS¹⁶ or by preparing standard samples of known composition.

As listed in Table 3a, the ingredients of the low-vulnerability propellants under study constitute of similar elements C-H-O and N, and similar molecules, making it difficult to differentiate the ingredients in the propellant by the conventional analytical methods. Degree of mixing analysis, however, require positive identification and differentiation of each ingredient in a given mixture.

On the other hand, as listed in Table 3b, the ingredients of this formulation exhibit distinct crystallinity characteristics: RDX (I) and β -HMX exhibit a unique crystal structure and plasticized CAB exhibits a unique amorphous structure. Our wide-angle x-ray diffraction technique then is a very effective method to differentiate and quantify the amounts of the ingredients present.

In this study, the relative volume fractions of the plasticized binder (CAB) and the fillers RDX + HMX, and "others" were calculated from the relative intensity fraction values which are unique to each ingredient. These measurements were carried-out utilizing a relatively high number of crystal-plane reflections of the crystalline powders (RDX and HMX) in order to eliminate texture effects and to increase accuracy (see Figure 3). For amorphous binder CAB, the entire broad amorphous peak (see Figure 3) was utilized.

A Rigaku DXR-3000 and a Siemens D-5000 computerized wide-angle diffractometer systems were used for these studies. In both systems, crystal monochromatized Cu K_{α} radiation at 40 KV and 20mA was applied. 0.15 and 0.6 degree receiving slits were used in all runs. The x-ray probe size was varied by using 1 degree and 0.5 degree primary beam slits and 5 mm diameter, 1 mm diameter and 0.3 mm diameter aperture windows made of lead. Thus, the effective x-ray probe sizes used were 0.1, 1 and 10 mm², respectively. The depth of penetration of the x-rays used in this technique was in the order of 0.5 mm. This depth was calculated according to¹⁴:

$$x = \frac{K_x \sin \theta}{2\mu} \quad (15)$$

where μ is the linear absorption coefficient ($\mu_{\text{LOVA}} = 12.4$ for Cu K_{α}), θ is beam angle (15°) and $K_x = 6.91$ for 99% of information. The experimental parameters of the x-ray diffraction experiments are summarized in Table 4.

RESULTS AND DISCUSSIONS

A typical wide-angle x-ray diffraction (XRD) pattern of the low-vulnerability propellant which constitute ~ 70% by volume RDX + HMX and ~ 30% CAB binder with additives, as obtained with Cu K α radiation, is shown in Figure 3a.

This is a convoluted pattern which includes diffraction peaks from all the ingredients present in the formulation. The ingredients present and the nature of their polyforms was first determined from these experimental diffraction patterns. Computer search/match and identification/elimination methods were applied utilizing the documented crystallographic data and XRD patterns listed in the JCPDS files¹⁶ and in the published literature.¹⁷ It was concluded that the propellants constituted RDX in RDX(I) polyform, HMX in β -HMX polyform and plasticized CAB binder in the amorphous form. The crystallographic information on the polyforms thus obtained are summarized in Table 3. The simulated diffraction patterns of crystalline RDX(I) and β -HMX are shown in Figures 3b and 3c, respectively. In Figure 3d, the XRD of the amorphous plasticized CAB is also shown to demonstrate the phase identification process.

Quantitative information on the volume fraction of the ingredients present was obtained from the XRD patterns by deconvoluting the relevant peaks of the ingredients. Standard samples of the raw ingredients, i.e., RDX + HMX powder, and plasticized CAB binder were prepared and utilized to calibrate the absolute values of the ingredient volume fractions. A sample pattern of quantitative analysis based on integrated peak computation is demonstrated in Figure 4. A XRD analysis software package i.e., Images by Rigaku, was used for quantitative studies. The contributions from the additives and the effects of the micro voids and strand perforations were omitted from these calculations.

The results of the quantitative x-ray diffraction analysis of relative volume fractions of plasticized CAB binder and RDX + HMX filler are shown in Figures 5 and 6, and Tables 5 and 6, for 10 mm² scale of examination, and in Figures 7 and 8, and Tables 7 and 8, for 1 mm² scale of examination, respectively. In all four figures and four tables the data from each of the four LOVA lots are juxtaposed for comparison.

Overall, the average volume fractions of the ingredients were relatively close to their target values in all four propellant lots. The deviations observed in the mean volume fraction values can be summarized as follows:

Plasticized CAB binder content was around 25 volume percent in three of the LOVA lots, i.e., Batch-45, Batch-54 and TSE-TH1, which is close to the targeted value of the master LOVA formulation. In lot TSE-IH-1, however, the plasticized CAB binder content was around 27 volume percent, 2% higher than the other three lots and the targeted formulation value. 2% increase in the binder content would noticeably affect the processing, degree of mixing

and possibly the performance of the given LOVA lot. Since the filler content is high in LOVA formulations, 2% by volume increase in binder content would make the processing easier and induce better mixing conditions. Higher binder content with good mixing would further lower the vulnerability of the LOVA lot, but would also decrease the energetic behavior. Furthermore, the opposite effects are expected when the binder content is lower, such as in the case of Batch-45.

RDX + HMX filler content was 1% to 2% by volume higher in the batch-mixed Batch-54 and Batch-45 lots than the continuously mixed TSE-TH1 and TSE-IH1 lots. The RDX + HMX content is inversely affected by the cumulative CAB and other ingredient contents. The RDX + HMX content of the Batch-54 and Batch-45 lots was about 1% higher than the targeted value; and the RDX + HMX content of the TSE-IH1 lot was about 1% lower than the targeted value.

A more striking difference between the lots was in the amplitude of the dispersion or variance of the relative volume fraction values. As can be seen in Figures 5 and 6, and Tables 5 and 6, the dispersion of the data is relatively narrow for 10 mm² scale of examination. However, when the scale of examination is reduced to 1 mm² (see Figures 7 and 8 and Tables 7 and 8) the dispersion of the data increase substantially and the differences in dispersion between the four lots increases significantly. The immediate inferences one can make from these results include the fact that the quality of mixing in TSE-TH1 and Batch-54 lots is better than the batch mixed Batch-45 lot, and TSE-IH1 lot falls in between.

How much better is, for example, TSE-TH1 lot from Batch-45 lot? The answer to this question can be found in the statistical parameters of the quantitative relative-volume-fraction measurements listed in Tables 5 through 8. For example, the parameters for the plasticized CAB relative-volume-fraction at 1 mm² scale of examination show that the dispersion or standard deviation of the data is almost twice as large for Batch-45 lot than TSE-TH1 lot. Since the mean values for the two lots are almost identical, the coefficient of variation (s/\bar{c}) is also twice as large for Batch-45 than TSE-TH1. The difference between the two lots is also evident in the amplitude or index of mixing ($1-s/s_0$) values. The relatively lower sensitivity of the index of mixing in differentiating the two lots is due, by definition, to its normalization with respect to the totally segregated state. The index of mixing value of 0.85 for Batch-45 lot, therefore, indicates the extensive amount of work that was put into the mixing process, even in this relatively inferior lot.

The subtle differences in the degree of mixing of those lots that exhibit similar variation parameters can be differentiated by studying the distribution characteristics of the variation parameters. An example of such a distribution-of-variation analysis is shown in Figure 7b, for CAB variation at 1 mm² scale. According to Figure 7b, the characteristics of the four lots in their distribution of CAB variation can be summarized as follows:

- the batch mixed and ram extruded lots Batch-54 and Batch-45 exhibit a distribution with a maximum frequency towards the higher plasticized CAB volume fraction (27%-30%), followed by a elongated tail towards the lower plasticized CAB volume fraction, indicating asymmetry (inhomogeneous) distribution. This inhomogeneity is most extenuated in Batch-45 which failed the burn test
- the twin screw extruded lots TSE-TH1 and TSE-IH1 exhibit a very limited asymmetric tail formation towards the lower plasticized CAB volume fraction

- however, in the batch-pre-blended and twin-screw extruded TSE-IH1 the CAB variation distribution exhibits an almost bimodal (two-peaks) characteristic with one maxima around 24% and another around 31%. Further analysis of the x-ray diffraction data revealed the origin of this bi-modality as coming from the variations from one grain (section) to another. Such large scale variations probably originate from the inadequacy of the batch-pre-blending process that was applied.
- In the twin-screw pre-blended and twin-screw extruded lot TSE-TH1, the distribution of CAB variation was almost unimodal, highly peaked and symmetric. This distribution characteristic of TSE-TH1 indicate homogeneous and narrow distribution and would make it a more reliable product with minimum surprises.

How significant are these results, which statistical parameter is more important and which scale of examination is more relevant? The answer to these questions can only come from the performance characteristics of the propellant for a given application. However, as demonstrated in this investigation, the technique and the parameters generated can accurately classify a given propellant with respect to ideally mixed and/or totally segregated states and quantify the "degree of mixing" of the propellant.

Furthermore, this investigation was carried out as a blind test, i.e., the comparative study was completed with no prior information about the four lots, and, only after presentation of the results some of the vital information was obtained from the sponsors. According to this information, the batch mixed Batch-45 lot, which exhibits the lowest degree of mixing in this investigation, had apparently failed the performance burn-test and was discarded. The other batch mixed lot, Batch-54, which exhibits one of the highest degree of mixing in this investigation, had passed the performance burn-test. Therefore, the results that are presented in this study are significant not only in determining the degree of mixing with quantitative parameters for evaluating the effectiveness of processing, but also screening for the potential performance of a given propellant. The results indicate that the relevant scale of examination is 1 mm² (or lower) for these "low vulnerability" propellants. Also, in order for a LOVA lot to pass the performance test, the index of mixing has to be significantly high (better than 0.90) at 1 mm² scale of examination with our x-ray diffraction technique.

Scanning electron microscopic (SEM) analysis were carried-out in order to assess qualitatively the microstructural features that give rise to the quantitative relative-volume-fraction values obtained with XRD measurements, and the consequent statistical parameters derived from these measurements. Typical micrographs obtained in Figure 9. As can be seen in photomicrographs, a, b, c and d of Figure 9, both the batch mixed and the continuous mixed propellants do exhibit regions which appear to be qualitatively homogeneous.

However, all four lots also exhibit regions that deviate from this relatively homogenous appearance. It is only the batch mixed Batch-45 lot, however, that shows the extreme case of binder deprived regions that is captured in photomicrograph of Figure 9e. The typical binder-deprived microstructure of Figure 9e was observed at those regions where the XRD measurements indicated binder content of less than 8% by volume at 1 mm² scale of examination in lot Batch-45. The XRD measurements, at the same scale of examination, did not show any such regions in other 3 LOVA lots. However, the preliminary x-ray measurements done at 0.1 mm² scale and the electron microscopy studies indicated that binder-deprived regions were present also in the Batch-54 samples, although at a much smaller scale than Batch-45. Such regions were not detected in the continuous processed

lots. The binder deprived pockets of RDX + HMX filler indicate inadequate mixing in Batch-45 lot, due to the processing conditions. One potential implication of the presence of unmixed RDX + HMX pockets during the "burning" of the propellant is the formation of reaction zones that are significantly different than the better mixed low-vulnerability regions, as targeted by the average formulation. This in turn could cause an unpredictable "burn" behavior of the propellant.

In the binder deprived regions of Batch-45 lot, the XRD measurements showed RDX + HMX relative-volume-fraction in excess of 90%. With the given particle size distribution, however, the theoretical packing density of the RDX + HMX powder cannot be more than 70% by volume, with the RDX powder synthesized at Indian Head, independent of the amount of the binder present. The theoretically calculated maximum packing density values was obtained by using numerical models at Stevens and will be reported separately.

With the given RDX powder with a maximum packing density of 70%: in some locations, the x-ray diffraction measurements show as little as 10% by volume CAB binder and as much as 90% by volume RDX + HMX filler particles. This generates a ratio of filler-to-binder which is as high as nine to one in the sampling volume. This result thus also indicates that there is interparticle void space, i.e., air in the extruded grains. Taking the void space into consideration, therefore, and assuming that the filler particle packing density is maximum, in the sample given, 70% is RDX + HMX filler particle, one-ninth of that, or 8% is binder plasticized CAB and the remaining 20% of the volume is interparticle micro void space filled with air or species from the process volatiles such as the solvents. In all those measurements that exhibit RDX + HMX relative volume fraction more than 70%, similar calculations can be carried-out to determine the micro-void space in the given specific volume of the propellant under examination. The x-ray diffraction technique can therefore, also measure quantitatively the micro-void space trapped inside the concentrated propellant which is otherwise difficult to access by other techniques.

The importance of the detection and control of larger void formation is demonstrated in Figure 10. Here the microvoids observed in two of the better mixed lots are shown. These microvoid pockets tend to be rich in plasticized binder and possibly originate from the use of excess solvent. As shown in Figure 10a and 10b, void formation was a persistent problem with TSE-TH1 lot. Large number of voids were distributed in a circular-band fashion clustered several hundred micrometers away from the strand surface.

CONCLUSIONS

1. Our degree of mixing analysis technique based on wide-angle x-ray diffraction which was developed earlier was applied to analyze RDX based low-vulnerability LOVA propellants.

2. Our technique has:

a) identified various components present in propellant formulation, i.e., plasticized CAB, RDX (α), HMX (β) and "others"

b) quantitatively determined the volume fraction for each component at various locations in propellant grains

c) quantitatively characterized the degree of mixing of each component at desired scale of examination, i.e., 0.1 mm², 1 mm² and 10 mm²

d) assessed the presence of interparticle microvoids in those cases where the RDX filler content exceeds the theoretical packing density of the RDX powder

3. Overall, the average volume fractions of the propellant ingredients were close to their target values in both batch mixed and continuous mixed lots. The detectable deviations were: higher plasticized CAB binder content of TSE-IH1; and, higher RDX + HMX content of Batch-54 and especially the Batch-45 lot.

4. The quality of mixing varied from one propellant to another and as a function of location for each propellant.

5. At larger scale of examination (10 mm²) the degree of mixing of the Batch-45 lot was marginally lower than the other three LOVA lots.

6. At smaller scale of examination (1 mm²) the quality of mixing of plasticized CAB and RDX + HMX was the highest in the continuous mixed TSE-TH1 lot followed by the batch mixed Batch-54 lot, and was lowest in the batch mixed Batch-45 lot. The TSE-IH1 lot exhibited a quality of mixing in between.

7. Small pockets (0.01 mm³ - 1 mm³) of binder deprived RDX rich regions were noticeably present in batch mixed Batch-45 and a much smaller scale in Batch-54 but were not detected in the continuously-TSE-processed lots.

8. In general, the variation coefficient and mixing index were effective parameters in quantifying degree of mixing and predicting the performance of low-vulnerability propellants.

FUTURE WORK

The following are recommended as future work to enhance the findings of this investigation:

- analysis of more LOVA lots, especially those which have exhibited significant and unexpected burning rate characteristics
- analysis of mixing distribution as a function of location in grain cross-section; i.e., at edges, perforations and bulk.
- analysis of microvoid formation/distribution by diffraction
- analysis of mixing distribution at smaller scales, i.e., 0.1 mm², 0.01 mm²
- systematic study of the effects of processing parameters on mixing distribution
- analysis of the effect of processing on RDX particle size distribution and particle defect structure
- analysis of the degree of crystallinity of energetic ingredients as affected by processing and formulation
- correlation of the field performance of propellants with the mixing distribution, degree of crystallinity and defect structure of energetic ingredients
- development of the x-ray diffraction technique as an on-line near real time quality control method for both batch and continuous energetics processing technologies
- development of a transportable x-ray unit that can be taken to various processing sites for on-site analysis of energetic materials

Table 1. LOVA formulation

| <u>Ingredient</u> | <u>Volume %</u> | <u>Density</u> |
|-------------------|-----------------|----------------|
| RDX+HMX | 68.38 | 1.79 |
| Plasticized CAB | 25.40 | 1.18 |
| "Others" | 6.26 | 1.15 |
| Total Dry | 100.00 | 1.58 |

Table 2. Mixing indices

mean:
$$\bar{C} = \frac{1}{N} \sum_{i=1}^N C_i$$

variance:
$$S^2 = \frac{1}{(N-1)} \sum_{i=1}^N (C_i - \bar{C})^2$$

standard deviation: S

coefficient of variation: $CV = S / \bar{C}$

mixing index: $MI = 1 - S / S_0$

maximum variance: $S_0^2 = \bar{C} (1 - \bar{C})$

intensity of mixing: $I_{mix} = 1 - S^2 / S_0^2$

intensity of segregation: $I_{seg} = S^2 / S_0^2$

segregation index: $SI = S / S_0$

Table 3a. LOVA Ingredients

| <u>Label</u> | <u>Name</u> | <u>Formula</u> |
|--------------|---|----------------|
| RDX | Cyclotrimethylene-trinitamine - (Hexogen or Cyclonite) | $C_3H_6N_6O_6$ |
| HMX | Octahydro - 1,3,5,7 - tetranitro - -1,3,5,7 - tetrazocine (Octogen) | $C_4H_8N_8O_8$ |
| CAB | Cellulose Acetate Butyrate | |
| | (.5) Cellulose | $C_6H_{10}O_5$ |
| | (.13) Acetyl | CH_3CO |
| | (.37) Butyryl | $CH_3(CH_2)_3$ |

Table 3b. Crystal Structure of LOVA ingredients

Name / Crystal Structure / Lattice Constants / Space Group / Density

| | | | | |
|---------|---------------------------|---------------|--------------|--|
| RDX (l) | Orthorhombic | | | |
| | $a = 13.19,$ | $b = 11.592,$ | $c = 10.714$ | (SG: Pbc _a) and |
| | $a = 11.61,$ | $b = 13.18,$ | $c = 10.72$ | (SG: Pcab) |
| | $d_x = 1.806$ and 1.801 | | | |
| HMX (b) | Monoclinic | | | |
| | $a = 6.537,$ | $b = 11.052,$ | $c = 8.702,$ | $\beta = 124.4$ (SG: P2 ₁ /c) |
| | $d_x = 1.538$ (Z= 2) | | | |
| CAB | Amorphous | | | |
| | $d = 1.2$ | | | |

Table 4. X-ray diffraction experimental parameters

| <u>Parameter</u> | <u>Value</u> |
|---------------------|--|
| KV | 40 |
| mA | 20 |
| monochromator | graphite crystal |
| diverging slit size | 1 deg., .5 deg. |
| soller slit size | 1 deg. |
| receiving slit size | .15 deg, .3 deg., .6 deg. |
| probe size | 0.1 mm ² , 1 mm ² , 10 mm ² |
| depth of peneration | 0.5 mm |

Table 5. Plasticized CAB statistical parameters at 10 sq.mm scale

| Relative Volume Fraction <u>Parameters</u> | LOVA | | | |
|--|-----------------|-----------------|----------------|----------------|
| | <u>Batch 54</u> | <u>Batch 45</u> | <u>TSE-TH1</u> | <u>TSE-IH1</u> |
| mean | 25.6 | 24.7 | 25.1 | 27.8 |
| standard deviation | 1.65 | 2.18 | 1.98 | 1.98 |
| coefficient of variation | .06 | .09 | .08 | .07 |
| mixing index | .96 | .95 | .95 | .96 |

Table 6. RDX+HMX statistical parameters at 10 sq.mm scale

| Relative Volume Fraction <u>Parameters</u> | LOVA | | | |
|--|-----------------|-----------------|----------------|----------------|
| | <u>Batch 54</u> | <u>Batch 45</u> | <u>TSE-TH1</u> | <u>TSE-IH1</u> |
| mean | 71.4 | 71.4 | 70.4 | 68.5 |
| standard deviation | 1.65 | 2.22 | 1.95 | 1.71 |
| coefficient of variation | .02 | .03 | .03 | .02 |
| mixing index | .96 | .95 | .96 | .96 |

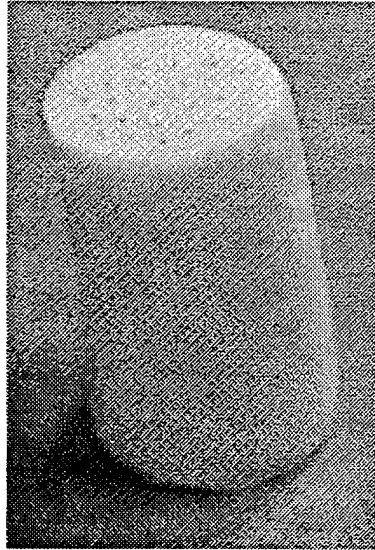
Table 7. Plasticized CAB statistical parameters at 1 sq.mm scale

| Relative Volume Fraction <u>Parameters</u> | LOVA | | | |
|--|-----------------|-----------------|----------------|----------------|
| | <u>Batch 54</u> | <u>Batch 45</u> | <u>TSE-TH1</u> | <u>TSE-IH1</u> |
| mean | 25.8 | 24.7 | 25.5 | 27.2 |
| standard deviation | 3.81 | 6.32 | 3.44 | 4.19 |
| coefficient of variation | .15 | .26 | .13 | .15 |
| mixing index | .91 | .85 | .92 | .90 |

Table 8. RDX+HMX statistical parameters at 1 sq.mm scale

| Relative Volume Fraction <u>Parameters</u> | LOVA | | | |
|--|-----------------|-----------------|----------------|----------------|
| | <u>Batch 54</u> | <u>Batch 45</u> | <u>TSE-TH1</u> | <u>TSE-IH1</u> |
| mean | 70.4 | 71.1 | 69.8 | 69.03 |
| standard deviation | 5.11 | 4.97 | 3.48 | 4.14 |
| coefficient of variation | .07 | .07 | .05 | .06 |
| mixing index | .91 | .89 | .92 | .91 |

(a)



(b)

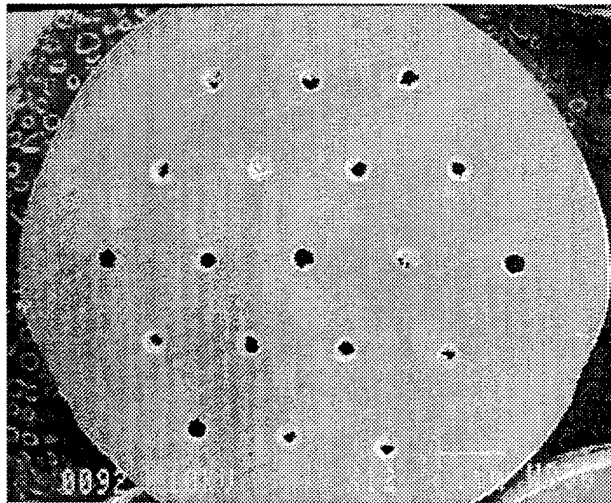


Figure 1. 0.3" dia. LOVA grain (a), transverse section (b).

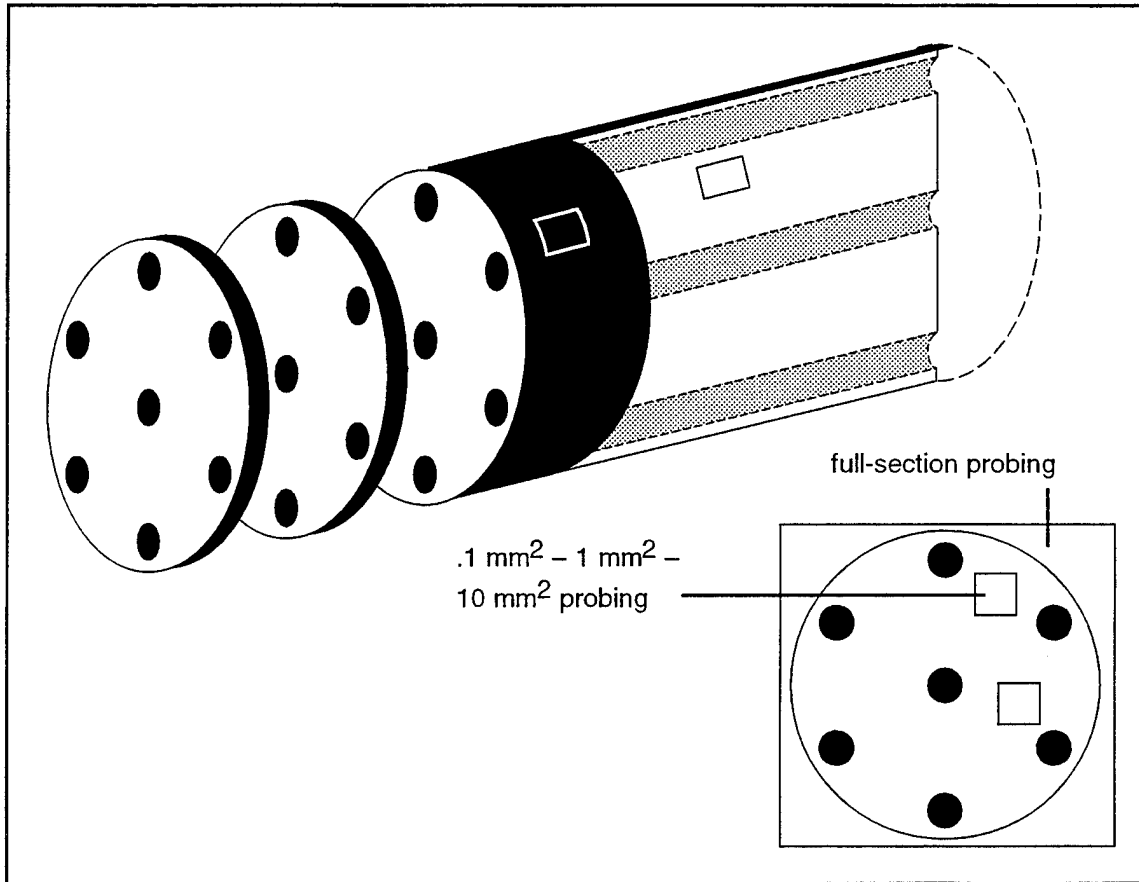


Figure 2. Extruded LOVA propellant: sampling and x-ray probe size.

Z00037.5AV
R.6.21 TL101-G2-TS:F2 1.1.6.6 2DPM

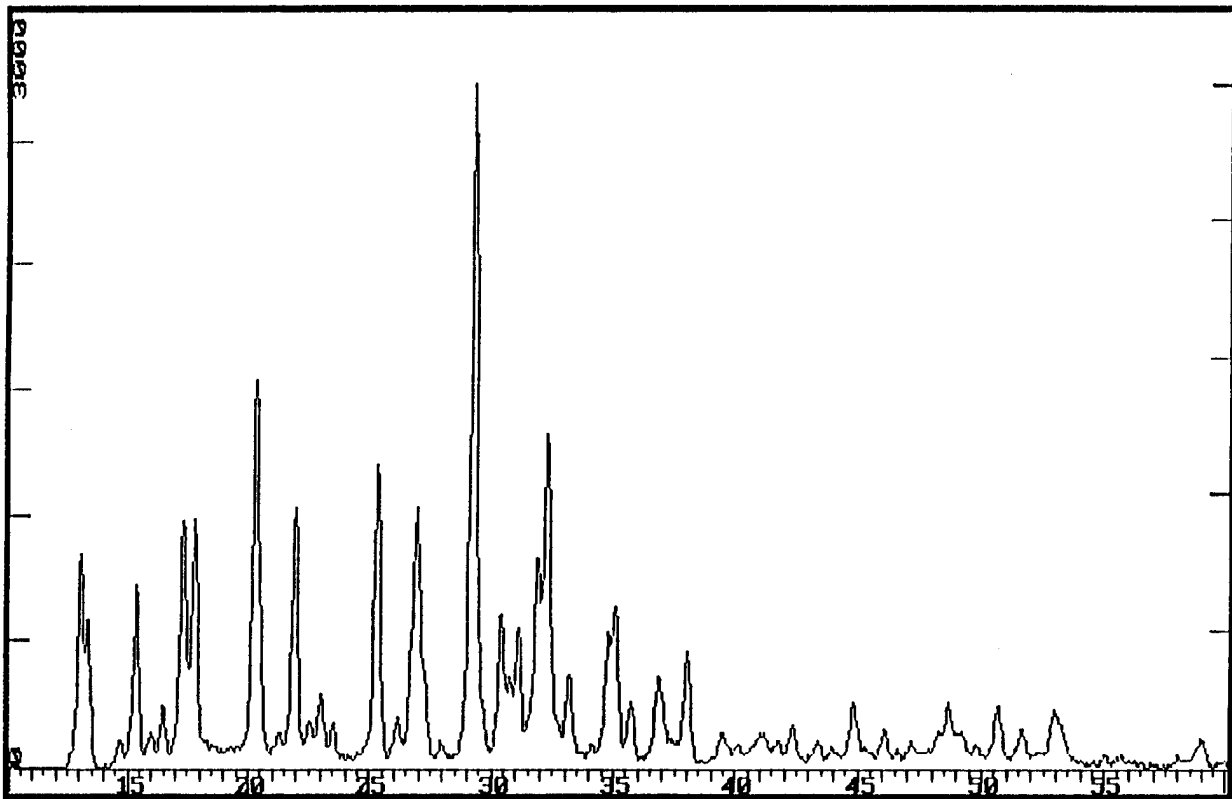


Figure 3. Typical x-ray diffraction pattern of LOVA propellants (a);

Z00064.SAV
R.6.26 TL-101-CAB+AIEC/SOLV 1.1.6 10D

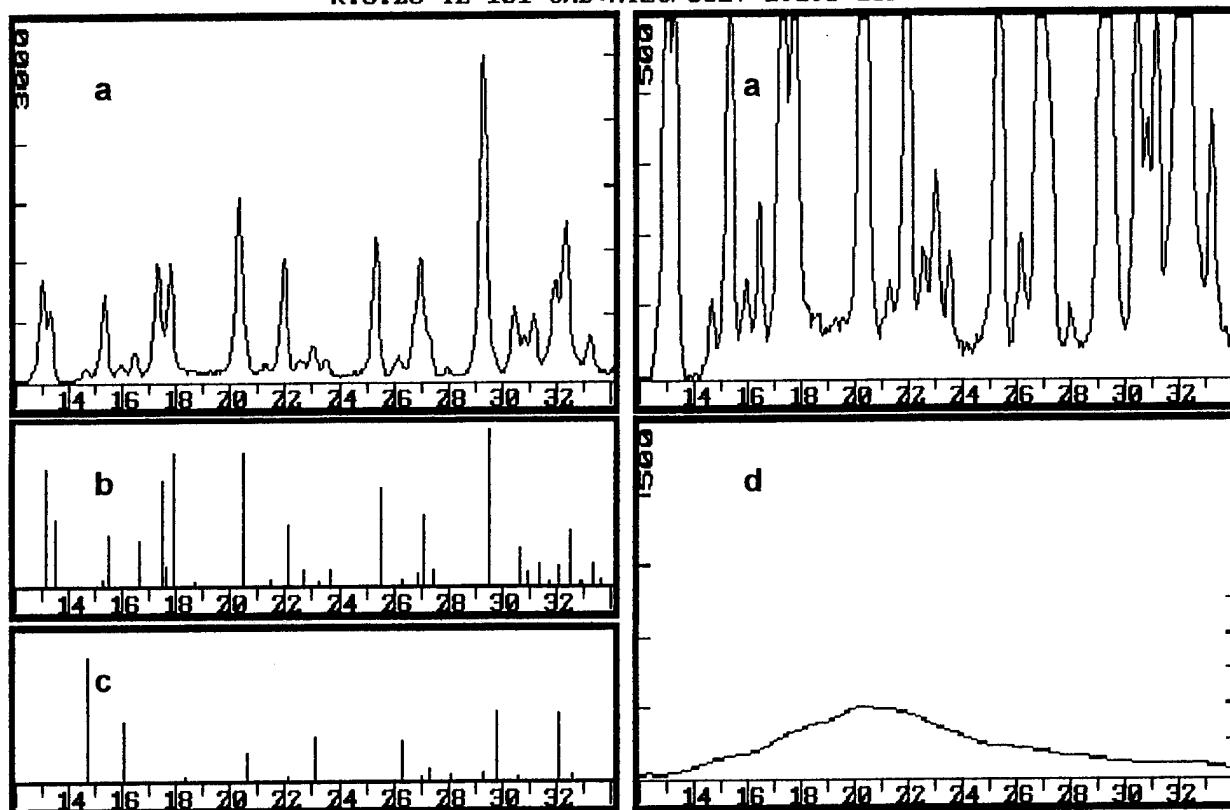


Figure 3. Typical x-ray diffraction pattern of LOVA propellants (a); simulated bar pattern of crystalline RDX (I) (b); simulated bar pattern of crystalline β -HMX (c); and amorphous peak of plasticized-CAB (d).

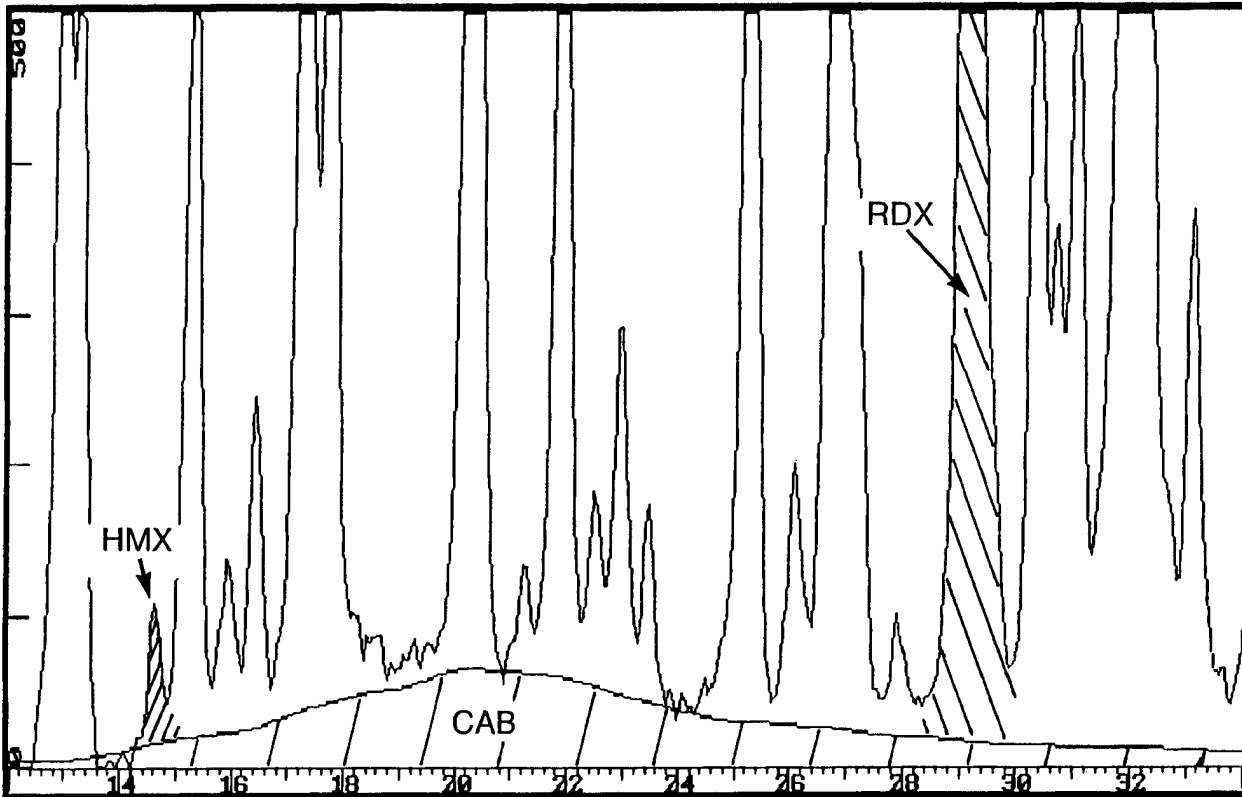


Figure 4. Deconvolution of a typical x-ray diffraction pattern of LOVA propellant where integrated areas of the peaks from different ingredients are marked.

Fig. 5. PLASTICIZED CAB VARIATION IN LOVA PROPELLANTS at 10 sq.mm scale

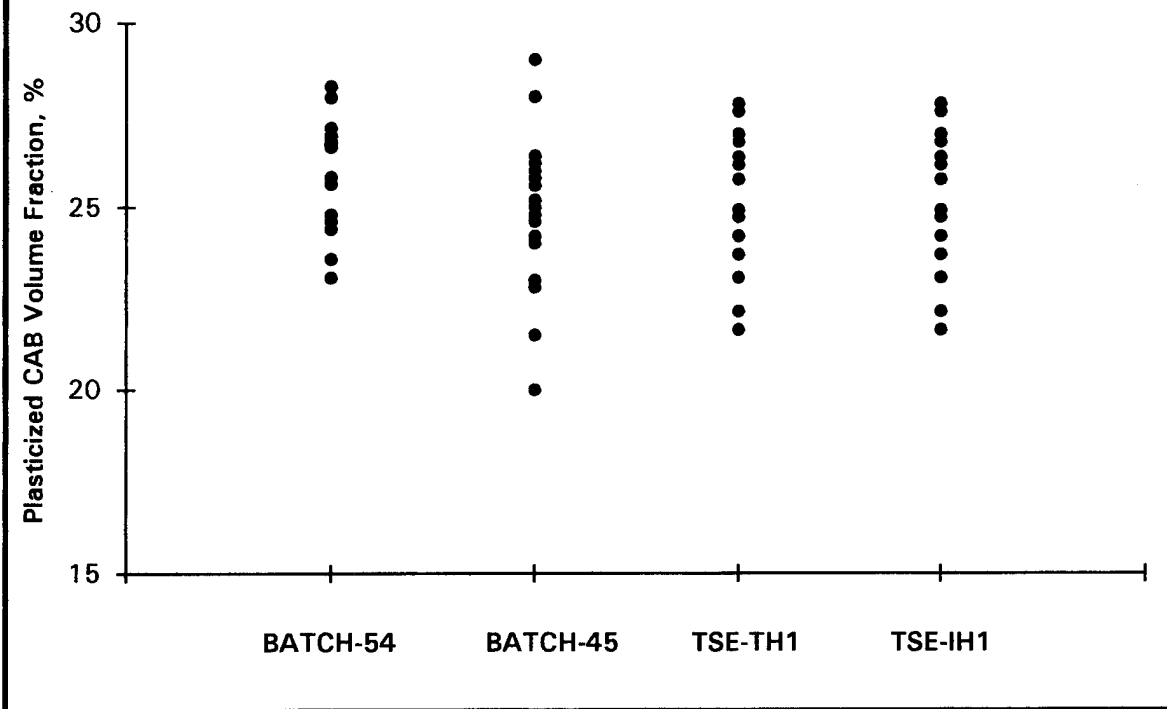


Fig. 6. RDX + HMX VARIATION IN LOVA PROPELLANTS
at 10 sq. mm scale

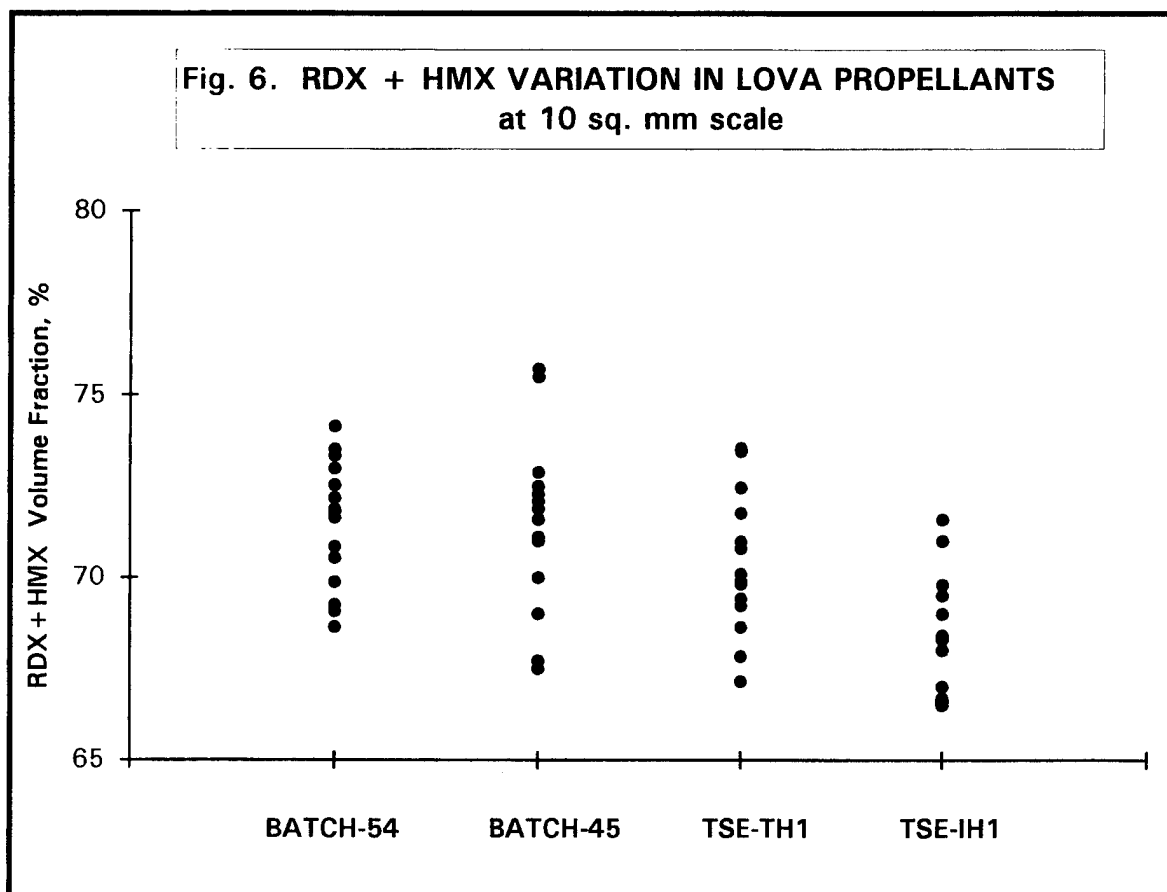


Fig. 7. PLASTICIZED CAB VARIATION IN LOVA PROPELLANTS at 1 sq.mm scale

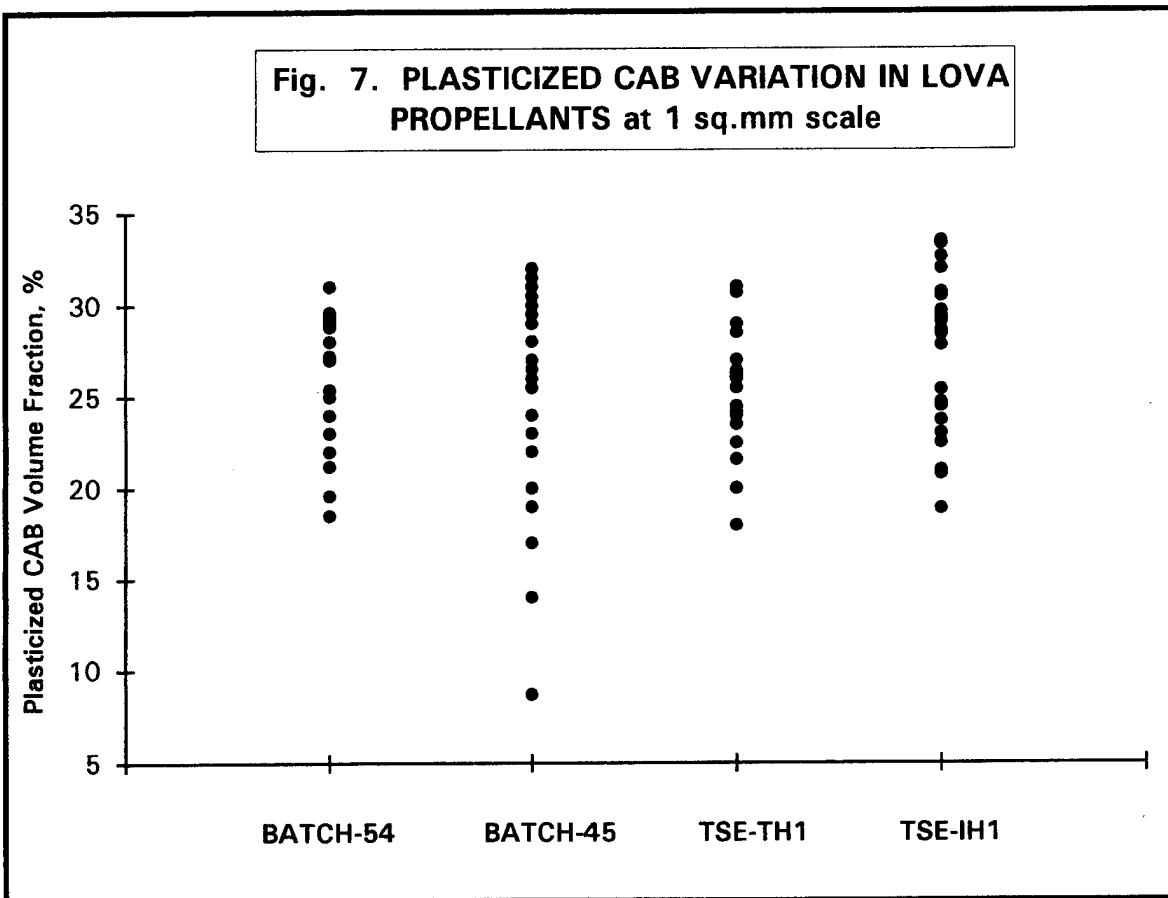


Fig. 7b. PLASTICIZED CAB VARIATION DISTRIBUTION in LOVA PROPELLANTS at 1sq.mm scale

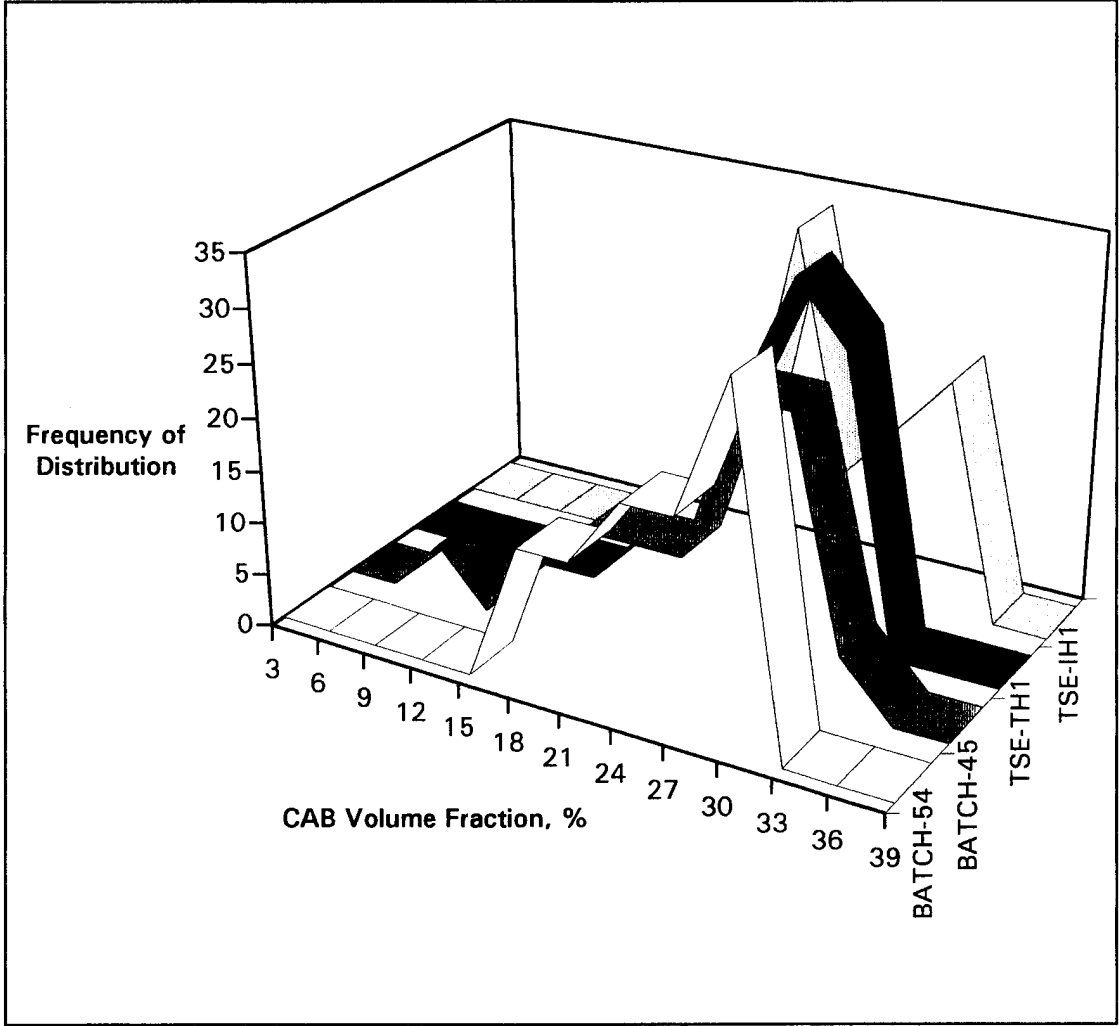
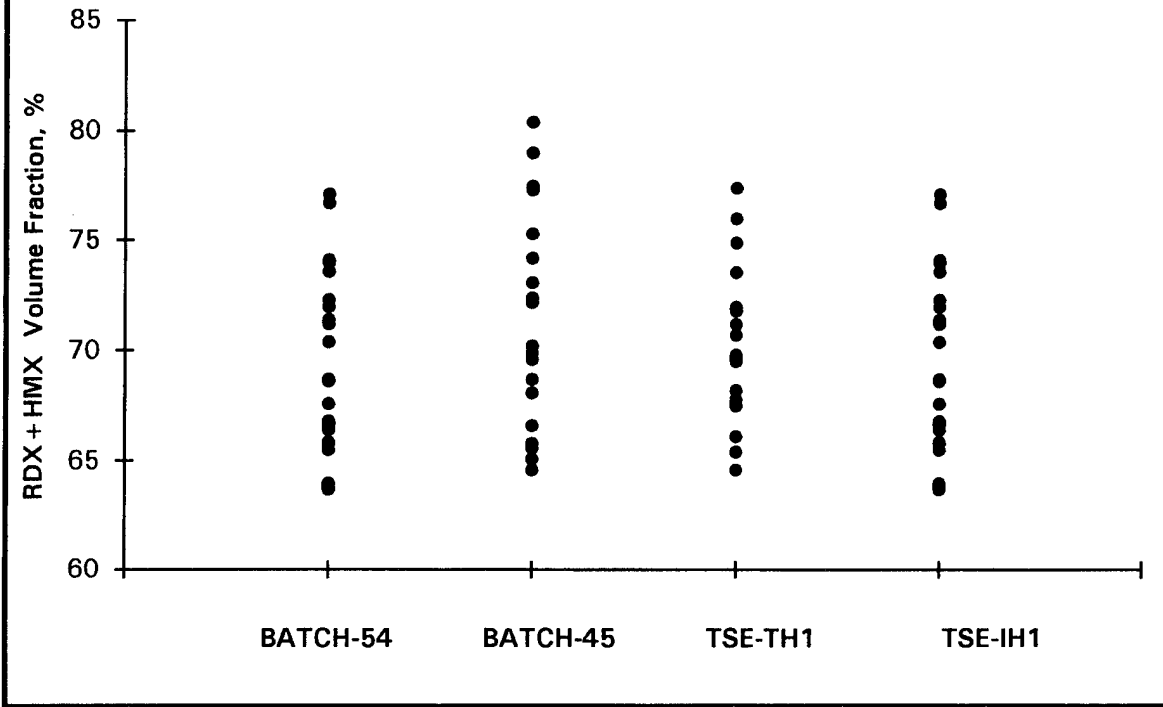


Fig 8. RDX + HMX VARIATION IN LOVA PROPELLANTS
at 1 sq. mm scale



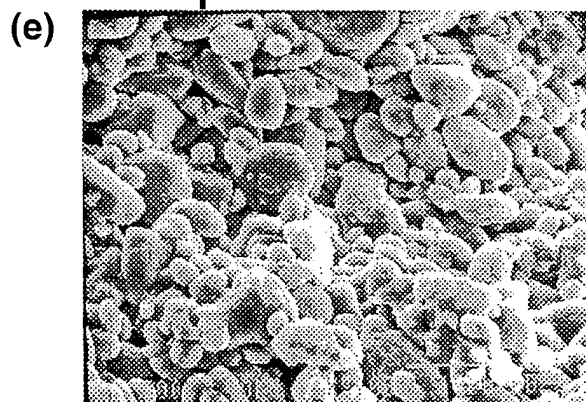
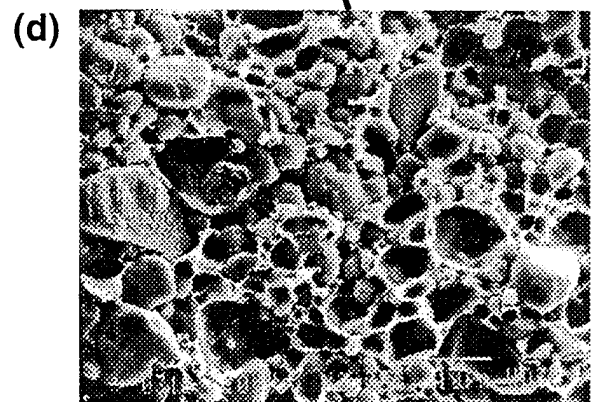
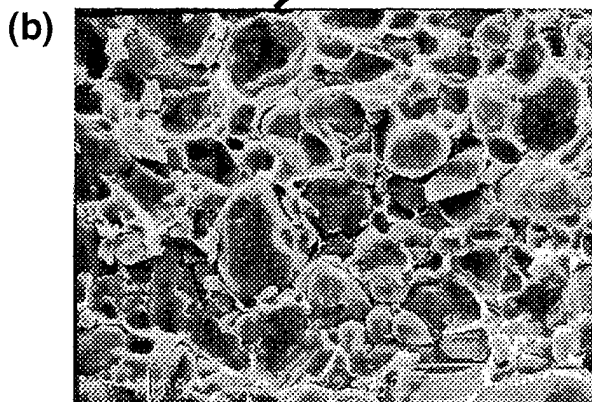
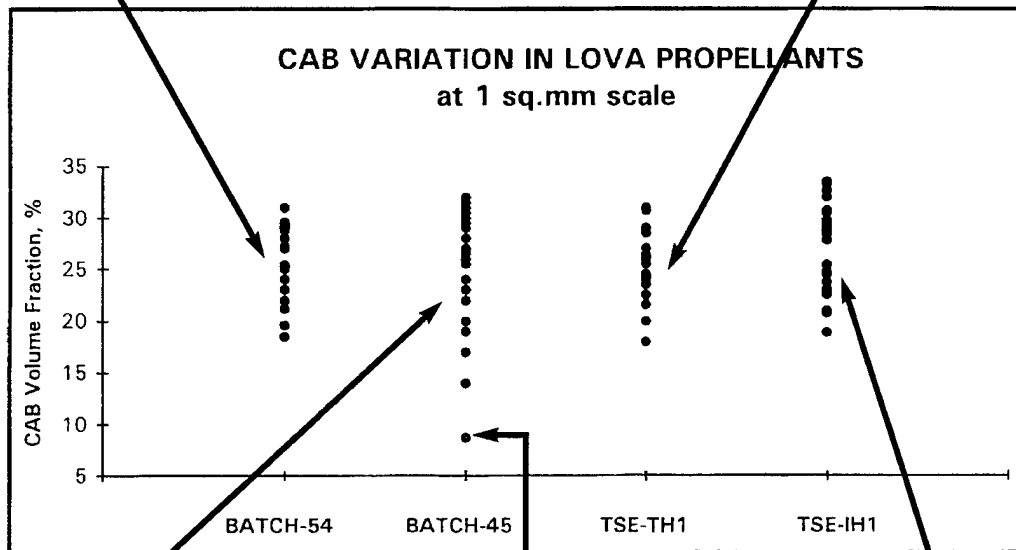
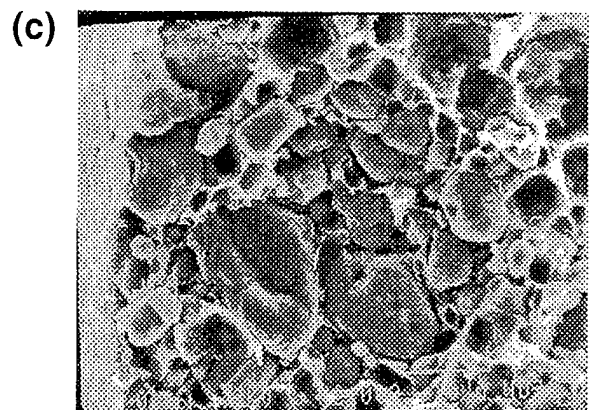
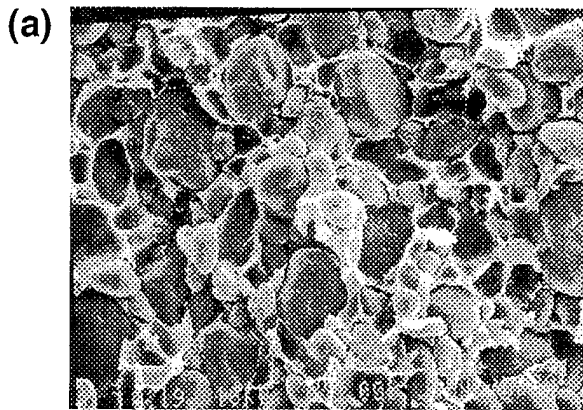


Figure 9. Typical microstructures of (a) Batch 54, (b) Batch 45, (c) TSE-TH1, (d) TSE-IH1, and (e) binder deprived RDX-rich region of Batch 45.

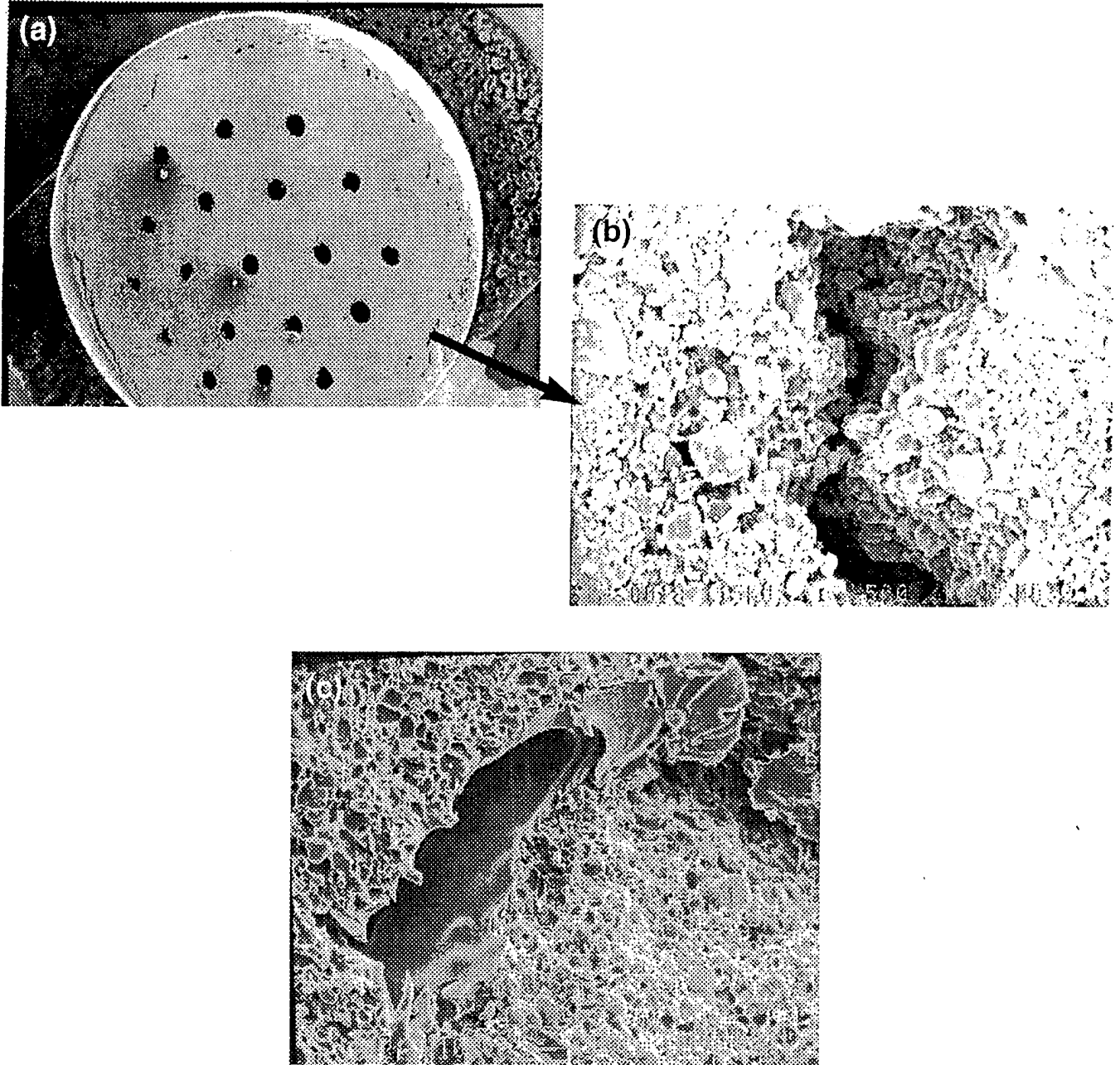


Figure 10. Microvoid defect formation in LOVA lots TSE-TH1 (a and b) and Batch 54 (c).

REFERENCES

1. Ottino, J. M., The Kinematics of Mixing: Stretching, Chaos and Transport, Cambridge University Press, 1989.
2. Morikawa, A., Min, K., and White, J.L., Int. Polym. Process, 4, p 23, 1989.
3. Rwei, S.P., Manas-Zioczower, I., and Feke, D. F., Polym. Eng. Sci., 30, p 701, 1990.
4. David, B., and Tadmor, Z., Int. Polym. Process, 3, p 38, 1988.
5. Gokboro, M. N., "Mixing in Single Screw Extruders," Ph.D. Thesis, University of Bradford, 1981.
6. Kubota, K., Brzoskowski, R., White, J. I., Weissert, F. C., Nakajima, N., and Min, K., Rubber Chem. Technol., 60, p 924, 1987.
7. Kalyon, D.M., Gotsis, A.D., Yilmazer, U., Gogos, C.G., Sangani, H., Aral, B., and Tsenoglou, C., Adv. Polym. Technol., 8, p 337, 1988.
8. Kalyon, D. M. and Sangani, H. N., Polym. Eng. Sci., 29, p 1018, 1989.
9. Kalyon, D. M., Yazici, R., Jacob, C., Aral, B., and Sinton, S.W., Polym. Eng. Sci., 31, p 386, 1991.
10. Yazici, R. and Kalyon, D. M., Rubber Chem. Technol., 66, p 527, 1993.
11. Kalyon, D. M., in Encyclopedia of Fluid Mechanics, Houston, TX, Gulf Publishing, Vol. 7, Ch. 28, pp 887-926, 1988.
12. Mohr, W.D., Processing of Thermoplastic Materials, E. Bernhard, Ed., Kreiger Publishing Co., Malabar, 1959.
13. Dieter, G. E., Engineering Design, McGraw Hill, New York, NY, 1983.
14. Cullity, B.D., Elements of X-Ray Diffraction, Addison-Wesley Pub., Reading, MA, 1986.
15. Alexander, L.E., X-Ray Diffraction Methods in Polymer Science, Kreiger Publ. Co., Malabar, 1985.
16. International Center for Diffraction Data, JCPDS Files, Swathsmore, PA, 1994.
17. Sullenger, D. B., Cantrell J.S., and Beiter, T. A., Powder Diffraction, 9, p 2, 1994.

DISTRIBUTION LIST

Commander
Armament Research, Development and Engineering Center
U.S. Army Tank-automotive and Armaments Center
ATTN: AMSTA-AR-IMC
AMSTA-AR-GCL
AMSTIO-IRA-W (6)
Picatinny Arsenal, NJ 07806-5000

Administrator
Defense Technical Information Center
ATTN: Accessions Division (12)
8725 John J. Kingman Road, Ste 0944,
Fort Belvoir, VA 22060-6210.

Director
U.S. Army Material Systems Analysis Activity
ATTN: AMXSY-MP
Aberdeen Proving Ground, MD 21005-5066

Commander
Chemical/Biological Defense Agency
U.S. Army Armament, Munitions and Chemical Command
ATTN: AMSCB-CII, Library
Aberdeen Proving Ground, MD 21010-5423

Director
U.S. Army Edgewood Research, Development and Engineering Center
ATTN: SCBRD-RTT (Aerodynamics Technical Team)
Aberdeen Proving Ground, MD 21010-5423

Director
U.S. Army Research Laboratory
ATTN: AMSRL-OP-CI-B, Technical Library
Aberdeen Proving Ground, MD 21005-5066

Chief
Benet Weapons Laboratory, CCAC
Armament Research, Development and Engineering Center
U.S. Army Armament, Munitions and Chemical Command
ATTN: SMCAR-CCB-TL
Watervliet, NY 12189-5000

Director
U.S. Army TRADOC Analysis Command-WSMR
ATTN: ATRC-WSS-R
White Sands Missile Range, NM 88002

GIDEP Operations Center
P.O.Box 8000
Corona, CA 91718-8000